A Comparison of GLDAS Soil Moisture Anomalies against Standardized Precipitation Index and Multisatellite Estimations over South America

PABLO C. SPENNEMANN

Centro de Investigaciones del Mar y la Atmósfera, Consejo Nacional de Investigaciones Científicas y Técnicas–Universidad de Buenos Aires, UMI–Instituto Franco–Argentino sobre Estudios de Clima y sus Impactos/CNRS, Buenos Aires, Argentina

JUAN A. RIVERA

Instituto Argentino de Nivología, Glaciología y Ciencias Ambientales (CCT-Mendoza/CONICET), Parque General San Martín, Mendoza, Argentina

A. CELESTE SAULO

Centro de Investigaciones del Mar y la Atmósfera, Consejo Nacional de Investigaciones Científicas y Técnicas–Universidad de Buenos Aires, UMI–Instituto Franco–Argentino sobre Estudios de Clima y sus Impactos/CNRS, Departamento de Ciencias de la Atmósfera y los Océanos, Facultad de Ciencias Exactas y Naturales, Universidad de Buenos Aires, and Servicio Meteorológico Nacional, Buenos Aires, Argentina

OLGA C. PENALBA

Departamento de Ciencias de la Atmósfera y los Océanos, Facultad de Ciencias Exactas y Naturales, Universidad de Buenos Aires and Consejo de Investigaciones Científicas y Técnicas, Buenos Aires, Argentina

(Manuscript received 26 November 2013, in final form 26 September 2014)

ABSTRACT

This study aims to compare simulated soil moisture anomalies derived from different versions of the Global Land Data Assimilation System (GLDAS), the standardized precipitation index (SPI), and a new multisatellite surface soil moisture product over southern South America. The main motivation is the need for assessing the reliability of GLDAS variables to be used in the characterization of soil state and its variability at the regional scale. The focus is on the southeastern part of South America (SESA), which is part of the La Plata basin, one of the largest basins of the world, where agriculture is the main source of income. The results show that GLDAS data capture soil moisture anomalies and their variability, taking into account regional and seasonal dependencies and showing correspondence with other proxies used to characterize soil states. Over large portions of the domain, and particularly over SESA, the correlation with the SPI is very high, with the second version of GLDAS, version 2 (GLDAS-2 v2), exhibiting the highest values regardless of the season. Similar results were obtained by comparing the surface soil moisture anomalies from the GLDAS land surface model (LSM) against the satellite estimations for a shorter period of time. This work documents that the precipitation dataset used to force each LSM and the choice of the LSM are of major relevance for representing soil conditions in an adequate manner. The results are considered to support the use of GLDAS as an indicator of soil moisture states and for developing new soil moisture–monitoring indices that can be applied, for example, in the context of agricultural production management.

1. Introduction

Soil moisture is a key variable of the earth–atmosphere system that not only reflects the soil conditions of a given region (e.g., as an indicator of agricultural droughts), but also influences the atmospheric variability from seasonal

Corresponding author address: Pablo C. Spennemann, Intendente Güiraldes 2160, Ciudad Universitaria, Pabellón II, C1428EGA Buenos Aires, Argentina.
E-mail: pspennemann@cima.fcen.uba.ar

DOI: 10.1175/JHM-D-13-0190.1

to synoptic time scales (e.g., Kanamitsu et al. 2003; Betts 2009; Seneviratne et al. 2010). Accurate observations and estimations of soil moisture are thus of high importance. In spite of this, global observational datasets (e.g., Robock et al. 2000) are very sparse in space and do not have temporal continuity over long periods of time. There are some exceptions over particular regions, as in the case of the Ukraine, North America (Robock et al. 2005), or China (Li et al. 2005). Many of these in situ measurements can be obtained through the International Soil Moisture Network (Dorigo et al. 2011; http://ismn.geo.tuwien.ac.at), which is a data hosting center where globally available ground-based soil moisture measurements are collected, harmonized, and made available to users. Still, observational data scarcity is a major issue that prevents the analysis of soil conditions, and it particularly stands out in South America, as shown by Seneviratne et al. (2010).

Land surface model (LSM) simulations are useful alternatives to analyze soil moisture variability. In particular, when LSM simulations are run uncoupled to an atmospheric model (e.g., forced with observations), they are devoid of biases generated by these models. Examples of this are the Global Soil Wetness Project, version 2 (GSWP-2; Dirmeyer et al. 2006); the Global Offline Land Surface Dataset, version 2 (GOLD-2; Dirmeyer and Tan 2001); and the Global Land Data Assimilation System, version 1 (GLDAS-1) and the first and second version of GLDAS, version 2 [GLDAS-2 v1 (no longer available) and GLDAS-2 v2, respectively; Rodell et al. 2004]. GLDAS uses multiple LSMs, comprises a longer period than other datasets, and provides different configurations where precipitation datasets used to force the LSM are changed. In this sense, GLDAS becomes valuable as a first approach to study soil moisture variability at regional scales, including the analysis of its representation by diverse models and forcings. Still, some kind of validation is desirable before using any model-driven product.

The lack of soil moisture observations limits the possibility to validate GLDAS at regional scales, such as, for instance, over South America. Nevertheless, a few in situ validations of GLDAS-1 were carried out. For example, Kato et al. (2007) performed an evaluation of four sites of the Coordinated Enhanced Observing Period (CEOP). They focused on the validation of 1 year of daily surface soil moisture from three different LSMs from GLDAS-1 and performed an intermodel comparison to highlight sensitivities to changes in precipitation, radiation, vegetation, and soil type. The authors observed that, in general, soil moisture is poorly represented by LSMs, and they attribute the discrepancies to differences between in situ observations and simulated soil depths. In their validation, soil moisture correlated well with precipitation and was more sensitive to precipitation during June–August (JJA) and September–November (SON) seasons. Their results also show important model dependency, highlighting that LSM choice is the most important influence on the simulation of water and energy partitioning. Another relevant evaluation of GLDAS was performed by Zaitchik et al. (2010) using global river discharge data and a source-to-sink routing scheme, proving their ability to simulate the water cycle process under different geographies and climate conditions. More recently, Xia et al. (2014) performed a validation of the North American Land Data Assimilation System, phase 2 (NLDAS-2), against Illinois and Oklahoma Mesonet. The authors documented that the different LSMs were capable to capture the seasonal and interannual variability of observed soil moisture.

Given our interest to assess GLDAS over South America, where a direct and long-term validation with in situ measurements is unfeasible, we confront the following question. What kind of dataset can be used to assess GLDAS soil moisture variability representativeness? A first alternative could be to compare GLDAS soil moisture variability against a well-known proxy of the water deficit/excess over land, like the standardized precipitation index (SPI). A second alternative could be a comparison against remote sensing estimations. Even though long-term multisatellite estimations may present some drawbacks, as will be explained later in the paper, they offer valuable information about surface soil moisture conditions. Using both datasets will provide complementary assessment, since the comparison with the SPI will disclose climatological aspects of GLDAS, given the possibility of long-term comparison. On the other hand, satellite estimations will account for physical processes (e.g., those related with soil and vegetation interactions) that are missing in the SPI.

The SPI was developed by McKee et al. (1993) for drought definition and monitoring, and it quantifies the number of standard deviations that accumulated rainfall in a given time scale deviates from the average value of a location in a particular period. The World Meteorological Organization (WMO) states that, in primary agricultural regions, a 3-month SPI (SPI3) might be more effective in highlighting available moisture conditions than other current hydrological indices (WMO 2012), and it has also been recommended by the Lincoln Declaration on Drought Indices (Hayes et al. 2011). Furthermore, the SPI was successfully used for comparison between precipitation and soil moisture indices in several regions of the world (e.g., Szalai et al. 2000; Ji and Peters 2003; Sims et al. 2002; Mueller and Seneviratne 2012). In particular, Mueller and Seneviratne (2012) used the SPI from

global precipitation datasets as a soil moisture deficit proxy for determining the influence of previous soil conditions on heat waves. They focused on the SPI3 and described the advantages of using SPI rather than estimations derived from satellite measurements, like the Soil Moisture Ocean Salinity (SMOS) or the Advanced Microwave Scanning Radiometer for Earth Observing System (AMSR-E). As with any proxy, pros and cons should be taken into account: the SPI is useful for describing surface moisture imbalances (Quan et al. 2012), but it does not consider nonlinear processes or evapotranspiration/gravity drainage that actually affect soil moisture.

Besides possible disadvantages of satellite estimations (e.g., nonstationary time series), important efforts are continuously being made to create long-term surface soil moisture estimations derived from satellite measurements. In this sense, a relatively new surface soil moisture product covering 1979–2010 has been derived that merges different passive and active microwave sensors [SM-MW, as presented in Wagner et al. (2012) and Liu et al. (2012) to indicate soil moisture microwave]. Despite these estimates only representing a thin superficial layer (from 1 mm to 2 cm) of the soil moisture content, which usually does not correspond to the LSM's superficial layer, they provide a reference and independent surface soil moisture variability estimation. For example, Dorigo et al. (2012) analyzed and compared the global soil moisture trends of the SM-MW product against the Interim European Centre for Medium-Range Weather Forecasts (ECMWF) Re-Analysis (ERA-Interim; Dee et al. 2011), GLDAS-1 Noah LSM, precipitation [Global Precipitation Climatology Project (GPCP); Adler et al. 2003], and the normalized difference vegetation index (NDVI; Tucker and Sellers 1986), for 1988–2010. The authors document that the major trends observed in SM-MW were also observed in the other datasets, with differences in the spatial extent. They also observed a strong drying tendency in all soil moisture products, which is not observed in the precipitation dataset. The authors also suggest that the effect of evaporation, vegetation, and soil type on soil moisture variations could be important, although precipitation is considered the main driver for the soil moisture variations. In Albergel et al. (2013), SM-MW temporal variability is compared to the land surface component of ERA-Interim (ERA-Interim/Land, hereinafter ERA-Land; Balsamo et al. 2012), an updated reanalysis version of ERA-Interim with focus on the soil/surface variables. Globally, the authors document that SM-MW is relatively stable compared to ERA-Land, with good agreement found especially in semiarid regions, while poor agreement is observed in tropical regions and in high latitudes.

Besides the necessity of drought monitoring and other applications that could be derived from better knowledge of soil moisture variability, it is also clear that agriculture producers would benefit from the availability of information on soil moisture amounts. In this context, the aim of this study relies on the need of assessing the representativeness of GLDAS-derived soil moisture anomalies over South America. We chose this dataset because it is the only one that encompasses the whole region and is consistent in terms of statistical properties. Our underlying hypothesis is that, if GLDAS soil moisture variability corresponds well with other proxies and/or measurements—generally accepted to describe soil conditions worldwide—then this dataset can be further employed to complement other descriptions of soil moisture at the regional level, where there is a lack of reliable measurements.

The evaluation of GLDAS soil moisture anomalies is carried out through their comparison with the SPI and SM-MW. On one side, this assessment will show how closely precipitation and soil moisture anomalies are related (from the model perspective). On the other side, it will show how closely these anomalies are compared to "direct" surface soil moisture estimations. Both assessments will also provide useful information regarding similarities and differences between the LSMs' behaviors over the region. These are the first steps needed to advance toward a more comprehensive validation using in situ measurements, since this study will not evaluate actual soil moisture amounts.

A special interest is set within an area inside southeastern South America, which is part of the La Plata basin (LPB), one of the largest basins of the world and reservoir of high biological diversity, where agriculture is the main source of incomes.

This work is structured as follows: section 2 describes data and methodology, section 3 exposes the results, and section 4 presents the discussion and main conclusions.

2. Data and methodology

Our study focuses on the southern part of South America (south of 20°S) and employs monthly values of GLDAS soil moisture from January 1980 to December 2008 and the Global Precipitation Climatology Centre (GPCC; Schneider et al. 2011) observational precipitation dataset, both with 1° × 1°grid spacing. The GPCC comprises 558 land grid points over the area of interest that were used to calculate the SPI over the same period.

The principal features of these datasets are detailed in Table 1, including the different LSMs, their corresponding soil layers, and the precipitation forcing datasets. The GLDAS system uses four LSMs: Noah;

TABLE 1. LSMs and data characteristics.

Product	LSM	Precipitation dataset used	Soil layers
GLDAS-2 v1	Noah, version 2.7 (v2.7; Chen et al. 1996)	Princeton University [Climatic Research Unit, version 2 (CRU2.0) + Tropical Rainfall Measuring Mission (TRMM) + GPCP + National Centers for Environmental Prediction–National Center for Atmospheric Research (NCEP–NCAR) reanalysis; Sheffield et al. (2006)]	4 (0–10, 10–40, 40–100, and 100–200 cm)
GLDAS-2 v2	Noah, version 3.3 (v3.3)		
GLDAS-1	Noah (v2.7)	Combination of CPC Merged Analysis of Precipitation (CMAP) + Global Data Assimilation System (GDAS) + ECMWF [see Rodell et al. (2004) for details]	4 (0–10, 10–40, 40–100, and 100–200 cm)
	Mosaic (Koster and Suarez 1996)		3 (0–2, 2–150, and 150–350 cm)
	VIC (Liang et al. 1994, 1996)		3 (0–10, 10–160, and 160–190 cm)
	CLM2 (Bonan et al. 2002)		10 (0–1.8, 1.8–4.5, 4.5–9.1, 9.1–16.6, 16.6–28.9, 28.9–49.3, 49.3–82.9, 82.9–138.3, 138.3–229.6, and 229.6–343.3 cm)
SPI		GPCC (Schneider et al. 2011)	

Common Land Model, version 2 (CLM2); Variable Infiltration Capacity (VIC); and Mosaic (Table 1). The main difference between the GLDAS versions is that GLDAS-2 (v1 and v2) is climatologically more consistent (driven by the global meteorological forcing dataset from Princeton University) than GLDAS-1. In other words, GLDAS-1 switches the forcing data sources several times over the record from 1979 to present, introducing unnatural trends (Rui and Beaudoing 2014). In turn, GLDAS-2 (v2) uses a new version of the Noah LSM that includes an improved snow parameterization and the land surface parameters are based on the Moderate Resolution Imaging Spectroradiometer (MODIS) and the Advanced Very High Resolution Radiometer (AVHRR) instead of using only the AVHRR as in GLDAS-1 and GLDAS-2 (v1). Following the recommendation of Rui and Beaudoing (2014), the period spanning 1995–97 was removed from GLDAS-1 because of high uncertainties in the forcing datasets used in the computation. Based on these datasets, we calculated the standardized soil moisture anomaly (SSMA) for comparison with the SPI.

The SPI is a powerful, flexible index that is simple to calculate and was widely used in southern South America, proving to be a good estimator of both wet and dry soil conditions (Seiler et al. 2002; Krepper and Zucarelli 2010; Penalba and Rivera 2013). It was designed to quantify the precipitation deficit for multiple time scales, which is essentially a standardized transformation of the probability of observed precipitation for any desired time scale duration (1, 3, 6, 12 months, etc.). A detailed description of the calculation of the SPI can be found in Lloyd-Hughes and Saunders (2002). Several approaches were used for comparison of the SPI with soil moisture indices. For example, Sims et al. (2002) compared normalized soil moisture and normalized SPI derived from in situ observations in North Carolina (United States). They conclude that short-term SPI (1–3 months) gives the highest correlation with 10-cm surface soil moisture and infer that deeper soil layers may show better correlation with longer time scales. They also conclude that the SPI can be used as a surrogate for obtaining soil moisture information. Ji and Peters (2003) assessed the vegetation response to drought in the United States using the NDVI. They suggested that the SPI on a time scale of 3 months is the best for determining drought severity and duration in vegetation cover, given the lag between precipitation and soil moisture deficits. In Hungary, Szalai et al. (2000) indicated that agricultural drought characterized by a decline in soil moisture content was better replicated by the SPI on a scale of 2–3 months.

The satellite soil moisture estimation, SM-MW, is a combination of several sensors, covering 1979–2010. The main features of SM-MW are shown in Table 2. Details of the merging technique and a complete description of the missions and sensors can be found in Wagner et al. (2012), Dorigo et al. (2012), and Liu et al. (2012). Nevertheless, it is important to highlight some characteristics of this dataset. For example, none of these sensors covers the entire period or provides complete spatial coverage, which is necessary for a global climate assessment. In turn, system retrieval algorithms and mission design differences entail a spatial and temporal variability of the data quality (Dorigo et al. 2012). A drawback of SM-MW for defining soil moisture amounts is that it uses climatological data from Noah

TABLE 2. SM-MW main features. DMSP is the Defense Meteorological Satellite Program, TMI is the TRMM Microwave Imager, SCAT is the European Remote Sensing Satellite (ERS) Scatterometer, and ASCAT is the Meteorological Operation (MetOp) Advanced Scatterometer.

	Passive microwave				Active microwave	
SM-MW	SMMR	SSM/I	TMI	AMSR-E	SCAT	ASCAT
Platform	*Nimbus-7*	DMSP	TRMM	*Aqua*	ERS	MetOp
Period	Jan 1979–Aug 1987	Sep 1987–Dec 2007	Jan 1998–Dec 2008	Jul 2002–Dec 2010	Jul 1991–Dec 2006	Jan 2007–Dec 2010
Channel	6.6 GHz (C band)	19.3 GHz (Ku band)	10.7 GHz (X band)	6.9–10.7 GHz (C and X band)	5.3 GHz (C band)	5.3 GHz (C band)
Units	$m^3 m^{-3}$	$m^3 m^{-3}$	$m^3 m^{-3}$	$m^3 m^{-3}$	Degree of saturation (%)	Degree of saturation (%)

GLDAS-1 to define the range of variability of estimated soil moisture. According to Liu et al. (2012), this only influences the absolute value of soil moisture and not the dynamics and trends of this variable. As it is also mentioned in Liu et al. (2012), the adjustment and combination of different sensors depends on the temporal overlap between them, which was hardly possible for the Scanning Multichannel Microwave Radiometer (SMMR) sensor (1979–87). These authors also conclude that the SM-MW is more reliable over periods where the estimates were obtained using C-band frequency sensors (see Table 2). In this sense, and based on a preliminary results (not shown), the period 1988–91 shows large uncertainty associated possibly with the Special Sensor Microwave Imager (SSM/I; Ku band), while the period 1992–96 shows significant changes in the variance compared with 1997–2008. Based on these results, we will use monthly averages only for 1997–2008.

The GPCC precipitation dataset used to construct the SPI has been first validated against observational data provided by the Europe–South America Network for Climate Change Assessment and Impact Studies in La Plata Basin (CLARIS LPB) project (Penalba et al. 2014). Figure 1 shows annual mean precipitation fields (1980–2008) and correlation coefficients between monthly time series of both datasets. It can be observed that the GPCC provides a good representation of precipitation amounts, in particular over the southeastern part of South America (hereinafter referred to as SESA; 35°–25°S, 63°–50°W). Over SESA, correlations are significant and generally higher than 0.7. In the southern part of the domain, there is also good agreement between datasets, but the lack of observations is notorious.

3. Results

a. GLDAS SSMA versus SPI

Given the various time scales in which precipitation and soil moisture interact, it is worthwhile to first perform a sensitivity analysis of the time scale of maximum correlations between the SPI and SSMA, in order to

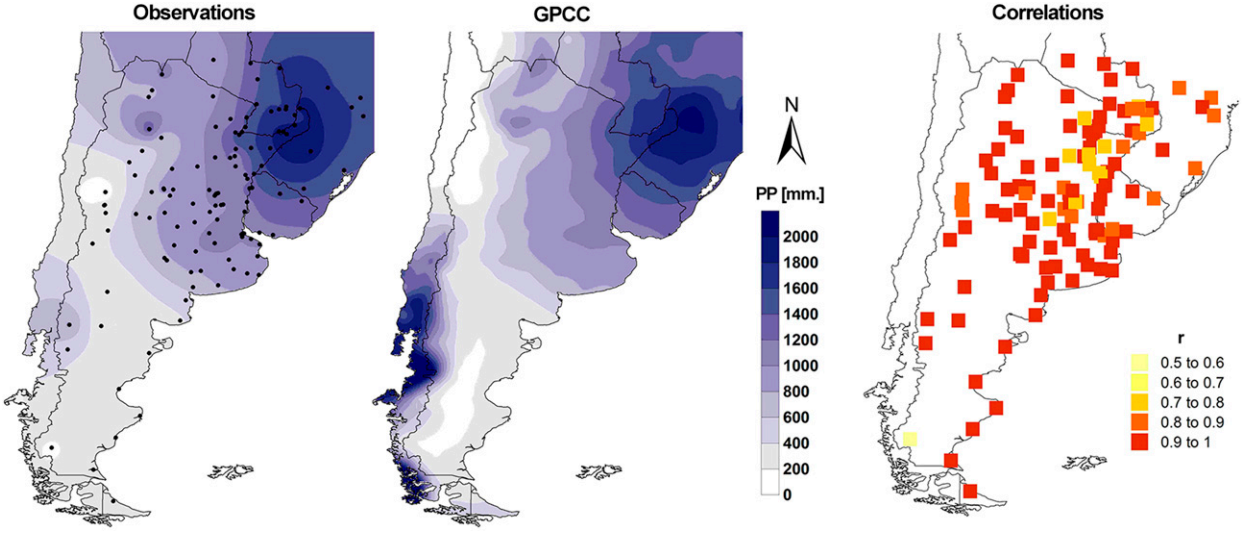

FIG. 1. Spatial distribution of (left) observed and (middle) GPCC annual precipitation, and (right) correlation coefficients between monthly time series of both datasets for the period 1980–2008.

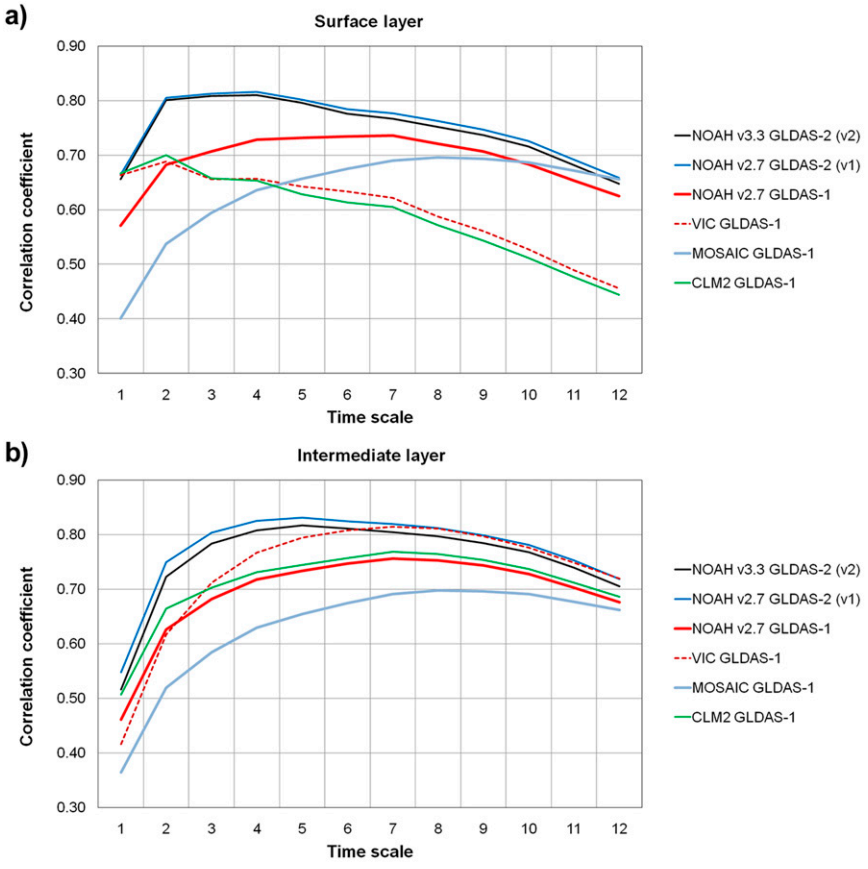

FIG. 2. Correlation between the SPI at different time scales and the SSMAs for all the LSMs in the (a) surface (see Table 1) and (b) intermediate layer (0–100 for Noah, 0–160 for VIC, 0–150 for Mosaic, and 0–138.3 cm for CLM2).

identify which SPI is more adequate for this study. Prior to the correlation computation, linear trends were removed to avoid spurious correlations. Figure 2 shows the correlation coefficients between the SPI—for 1–12-month time scales—and monthly SSMA from different GLDAS/LSMs. At the most superficial layer (Fig. 2a), high correlations ($r > 0.8$) are found for time scales between 2 and 5 months for both versions of GLDAS-2. Different model responses with SPI time scale are apparent: maximum correlation values occur earlier for VIC and CLM2 and considerably later for Mosaic. There are also diverse responses among Noah LSM versions, although the functional dependence with SPI time scale is similar. The origin of these discrepancies is hard to explain without going into parameterization details, which is out of the scope of this analysis. For example, CLM2 and VIC exhibit strikingly similar responses, but CLM2 represents a thinner surface layer than VIC. In turn, Mosaic and CLM2 show an opposite behavior with respect to the SPI, although they represent similar surface layer depths, and something similar happens if VIC and Noah are compared (at least for the first 6 months or so). This figure suggests that the superficial layer does not exhibit consistent behavior among models with respect to the SPI and that it may not be appropriate for our purposes (e.g., the assessment is too model dependent).

When deeper soil depths are considered (Fig. 2b), as expected, correlations tend to peak at longer time scales and the LSM response is more coherent, with maximum correlations around 4- and 5-month SPI (SPI4 and SPI5, respectively) for GLDAS-2. Comparing both figures, GLDAS-2 maintains a similar relationship with SPI time scales regardless of layer depth, but this is not the case for the other datasets. This result shows that an individual analysis is needed before defining which SPI should be used, since this will depend on each model and layer depth. To provide further arguments to support our choice of one SPI, the correlation seasonal dependence at the intermediate layer is presented. Table 3 highlights that the SPI3 shows the closest relationship with SSMA in summer and SPI4 in autumn. Taking into

TABLE 3. Seasonal correlation coefficients between SSMA and SPI at different time scales [3-, 4-, 5-, 7-, 8-, 9-, and 10-month SPI (SPI3, SPI4, SPI5, SPI7, SPI8, SPI9, and SPI10, respectively)] over SESA. The SPI time scale with the highest correlation coefficient (in parentheses) is indicated for every LSM and season considered.

LSM and GLDAS version	SSMA depth (cm)	Summer (DJF)	Autumn (MAM)	Winter (JJA)	Spring (SON)
Noah v3.3 GLDAS-2 v2	0–100	SPI3 (0.89)	SPI4 (0.88)	SPI5 (0.79)	SPI7 (0.81)
Noah v2.7 GLDAS-2 v1	0–100	SPI4 (0.88)	SPI4 (0.88)	SPI7 (0.82)	SPI8 (0.83)
Noah v2.7 GLDAS-1	0–100	SPI3 (0.82)	SPI4 (0.83)	SPI7 (0.79)	SPI8 (0.79)
VIC GLDAS-1	0–160	SPI4 (0.89)	SPI5 (0.90)	SPI7 (0.88)	SPI8 (0.86)
Mosaic GLDAS-1	0–150	SPI9 (0.73)	SPI5 (0.79)	SPI8 (0.77)	SPI10 (0.73)
CLM2 GLDAS-1	0–138.3	SPI3 (0.83)	SPI4 (0.87)	SPI8 (0.82)	SPI8 (0.83)

consideration that, from an agricultural point of view, SESA is a region of many summer and autumn crops (e.g., soy, wheat, and sunflowers; Andrade and Sadras 2000), we consider that the SPI3 can be used as a reference dataset for this evaluation. This choice is in agreement with previous studies like Szalai et al. (2000), Ji and Peters (2003), Mueller and Seneviratne (2012), among others. Moreover, for applications concerned with superficial soil layers (e.g., comparison with satellite estimates), the SPI3 exhibits the largest correlation with respect to GLDAS-2 SSMA. Note that the Noah GLDAS-2 v1 and v2 are the most consistent datasets in terms of their functional dependence with the SPI at different layers. The following discussion focuses on GLDAS-2 and its comparison with the other datasets for soil depths as shown in Fig. 2b (0–100 cm for Noah, 0–138.3 cm for CLM2, 0–150 cm for Mosaic, and 0–160 cm for VIC).

Previously, GLDAS-2 v1 and v2 were identified as the datasets with higher correlation with the SPI at diverse time scales, including 3 months (i.e., SPI3). Important differences between LSMs show up, some of which may be related with the use of different forcing datasets (e.g., GLDAS-2 v1 and GLDAS-1). To address this question, GLDAS-1 and GLDAS-2 precipitation fields are compared with GPCC data. Figure 3 shows that their relative differences with respect to GPCC have similar spatial patterns and are larger over the Andes and in the southern tip of the continent. Over SESA, these differences are mostly positive and do not exceed 30%. The anomaly correlation between GPCC and GLDAS-2 is higher than that for GLDAS-1, and this is mostly explained by a better representation of precipitation variability. This figure shows that GLDAS-2 precipitation forcing is more representative of the observations, in agreement with previous findings (Spennemann and Saulo 2014, manuscript submitted to *Int. J. Climatol.*), and further supports our choice of GLDAS-2 as a reliable estimate of surface states among those analyzed in our region of study.

Figure 4 shows the spatial pattern of the correlation between the SPI3 and simulated SSMA from all available datasets included in Table 1 and for the full period. The highest correlations are obtained with both versions of GLDAS-2 that depict more than 97% of the grid points with significantly positive values. Despite slight differences, the LSMs exhibit regional coherence and spatial patterns resemble those obtained for the correlation between GPCC and GLDAS precipitation, locating maximum values in central SESA. In particular, GLDAS-2 v2 shows the highest values over this area. Among GLDAS-1 LSMs, the highest correlations are obtained with the Noah and VIC, followed by CLM2 and Mosaic, which is in agreement with Fig. 2b. Minimum correlation coefficients were found over arid and mountainous regions.

Similarity of correlation patterns between Figs. 3 and 4 highlights the importance of precipitation as the main driver of simulated soil moisture anomalies. Higher correlations with both GLDAS-2 versions might be related with the fact that precipitation data used in GLDAS-2 and in the SPI are much alike.

Given the precipitation seasonality in southern South America and, therefore, in soil moisture and crops, the correlations at different seasons have been analyzed. Figure 5 shows the correlation coefficients using Noah GLDAS-2 v1, Noah GLDAS-1, and Mosaic GLDAS-1 for each season. This choice seeks to highlight the seasonal response if the same LSM is used but the forcing dataset is changed (e.g., comparison of GLDAS-2 and GLDAS-1) and if the same forcing dataset with different LSMs is used (Mosaic was selected because VIC and CLM2 correlations were too similar to Noah). For these LSMs, the highest correlation coefficients are observed over SESA in summer and autumn, followed by spring. With changing seasons, the areal coverage of high correlation values decreases and is at minimum in winter. This behavior is replicated by all the LSMs, suggesting the impact of the precipitation seasonal cycle on these correlations and illustrating the results already shown in Table 3 (e.g., correlation with the SPI tends to peak at longer time scales as the year progresses). Comparing the results for both datasets using Noah (GLDAS-2 v1

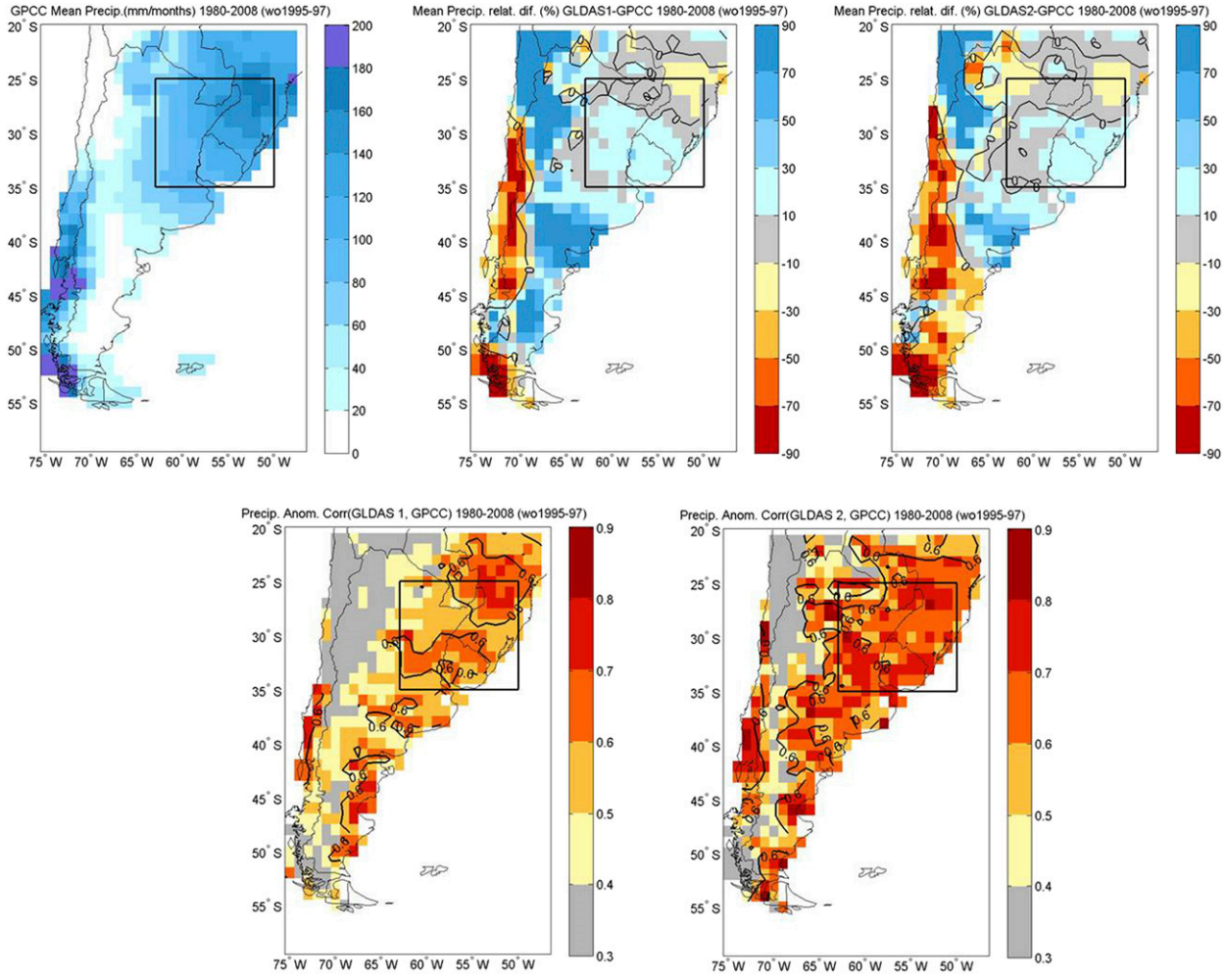

FIG. 3. (top left) GPCC mean precipitation (mm month^{-1}). Relative difference (%) of (top middle) GLDAS-1 and (top right) GLDAS-2 compared to GPCC, and (bottom) temporal correlation of the precipitation anomalies. Years 1995–97 have been disregarded (see text for details).

and GLDAS-1), it becomes clear that precipitation, as mentioned before, is a key input for LSM response, giving higher correlations whenever precipitation datasets are similar. Meanwhile, Noah and Mosaic correlation coefficients show similar spatial patterns, but with important differences in their magnitude, emphasizing the impact of using one LSM or another, as indicated by Kato et al. (2007).

Figures 6a and 6b show the areal averaged temporal evolution of the SPI3 and the two SSMAs of GLDAS-2 v2 and VIC between 1980 and 2008. This result underlines the resemblance between both time series variability. In particular, very good agreement is observed for the extreme drought that took place during 1988–89 over the region. Figure 6c shows the temporal evolution of the SPI3 and the SSMA of CLM2 and Mosaic over SESA. Despite the fact that both LSMs are able to capture excess and deficit periods, the magnitude shown by Mosaic is smaller in comparison with CLM2.

b. *GLDAS SSMA versus SM-MW*

The variability of SM-MW surface soil moisture estimations, averaged over SESA for 1997–2008, is shown in Fig. 7. The noise associated with the estimation and the mean monthly percentage of grid points with data are also shown. It is clear that, depending on the period of analysis, the percentage of grid points with data is lower than 10%. In addition, the magnitude of errors related to the estimation itself changes over time, as mentioned in Dorigo et al. (2012). It is interesting to draw the attention to the last period, where the highest estimation errors are observed in combination with the highest percentage (near 50%) of grid points with data. As in the previous section, where a comparison against a soil

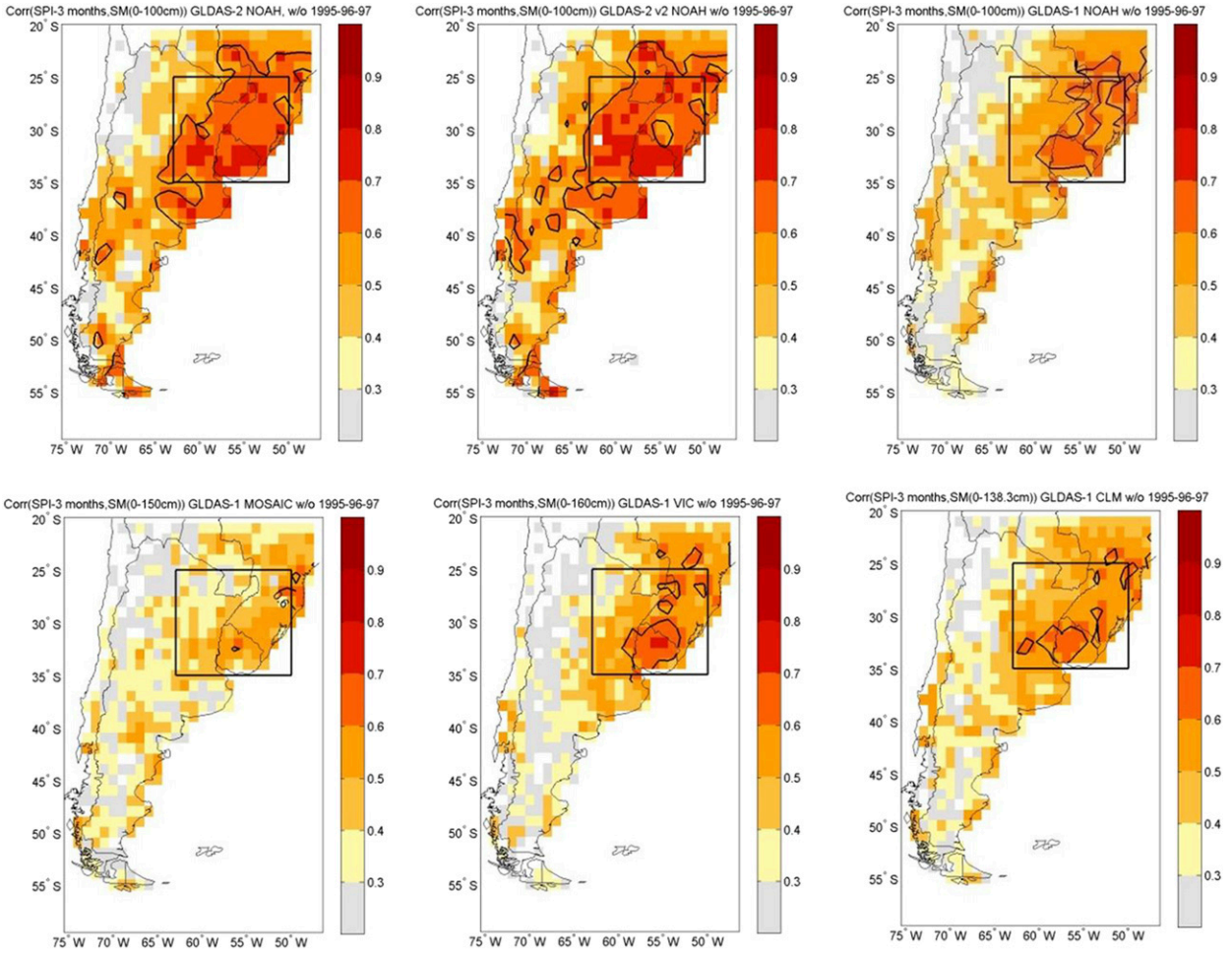

FIG. 4. Correlation (significant at 0.01 level; shaded) between SSMA from the different LSMs and the SPI3 for the full period (1995–97 have been disregarded; see text for details): (top left) GLDAS-2 v1, (top middle) GLDAS-2 v2, (top right) GLDAS-1 Noah, (bottom left) GLDAS-1 Mosaic, (bottom middle) GLDAS-1 VIC, and (bottom right) GLDAS-1 CLM2. Contour line denotes correlations of 0.6.

moisture condition proxy was carried out, in this case the representativeness of this estimation must also be taken with caution, given the lack of sustained coverage.

To compare this estimate of soil moisture variability with that obtained with different LSMs from GLDAS, the surface layer from each LSM (see Table 1) was chosen. In Fig. 8a the temporal series of GLDAS-2 v2, Noah GLDAS-1 surface layer SSMA, and SM-MW are shown. In general, GLDAS-2 v2 and Noah GLDAS-1 show a similar behavior compared with SM-MW, except for 2002–03.

Figure 8b shows GLDAS-1 Mosaic, VIC, and CLM2 in comparison with SM-MW. In general, GLDAS-1 LSMs show larger differences for 2007–08, as was also observed in Fig. 6 (i.e., compared with the SPI3). Furthermore, as it was observed from the comparison against SPI3, Mosaic also shows the largest differences compared with SM-MW estimations. During 2002–03, all the LSMs show a relative maximum, while SM-MW shows a relative minimum. This opposite behavior could be related with errors in the LSMs (although they reflect the same as the SPI3) or with a lack of representativeness of SM-MW data, given the lack of information during this specific period.

Table 4 summarizes SSMA variability for the different LSMs and their correlation with the SM-MW. It is interesting to mention that Noah GLDAS-1 and GLDAS-2 v2 show the highest correlation ($r = 0.71$), while Mosaic presents the lowest values. In terms of SSMA variability, all LSMs show similar values to SM-MW estimations. In particular, the VIC shows the lowest variability.

4. Concluding remarks

Motivated by the need to use a reliable soil moisture dataset to document the climatology and variability at diverse time scales over South America, an assessment

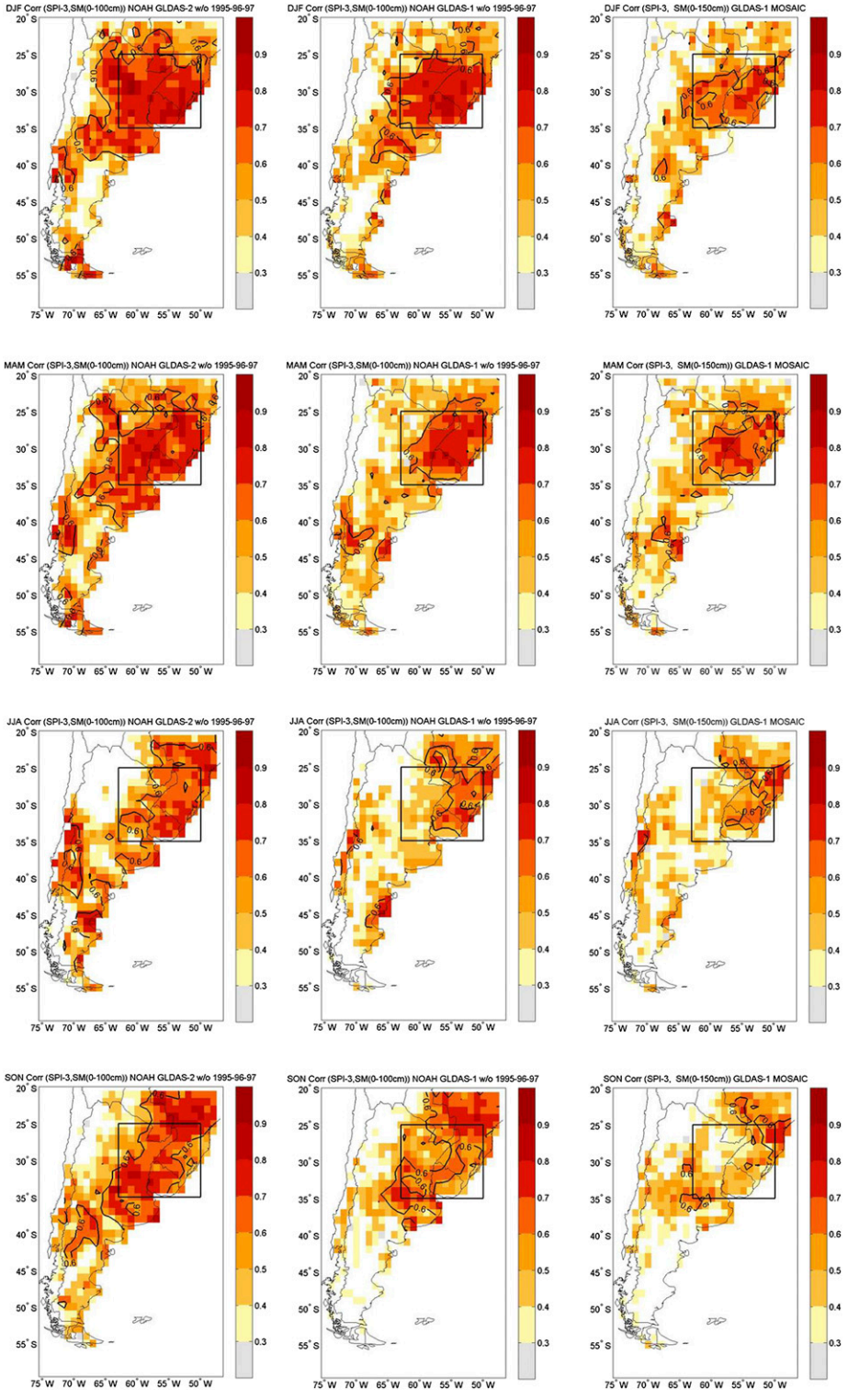

FIG. 5. Correlation (significant at 0.01 level; shaded) between SSMA from (left) GLDAS-2 v1 (Noah v2.7), (middle) GLDAS-1 Noah v2.7, and (right) GLDAS-1 Mosaic against SPI3 for (first row) summer [December–February (DJF)], (second row) autumn [March–May (MAM)], (third row) winter (JJA), and (fourth row) spring (SON). Contour line denotes correlations of 0.6.

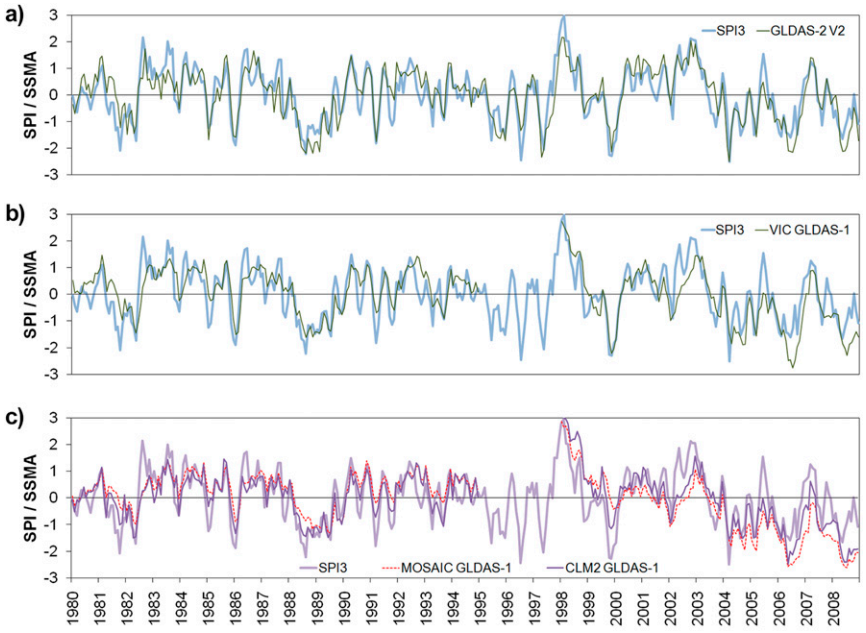

FIG. 6. Temporal series of (a) SPI and GLDAS-2 v2 SSMA (0–100 cm), (b) SPI and GLDAS-1 VIC (0–160 cm), and (c) the difference of three LSMs from GLDAS-1 (Noah, CLM2, and Mosaic) with respect to VIC, area averaged over SESA (35°–25°S, 63°–50°W).

of various GLDAS datasets, including distinct forcings and LSMs, has been carried out. Our underlying hypothesis was that GLDAS-2 (Noah LSM) would provide the most appropriate dataset, given that a climatological consistent atmospheric forcing was used to run this LSM during the period of analysis. The other hypothesis was that the standardized precipitation index, widely accepted as a measure to monitor droughts, could be employed as a proxy for soil water excess/deficit, and as such, its variability would go along with that of soil moisture. As the SPI does not consider important processes affecting soil moisture, like evapotranspiration or gravity drainage, a complementary multisatellite soil moisture estimation product (SM-MW) was used to improve the analysis.

While doing so, it is implied that only modeled soil moisture anomalies would be evaluated against the SPI and SM-MW, since there is no possibility to compare soil moisture amounts.

After validating precipitation fields used to force the LSMs, it has been shown that GLDAS-2 precipitation is in better agreement with the observations. Another interesting analysis arose from the comparison between the SPI at various time scales and soil moisture anomalies from different LSMs and layers, with a focus over SESA. Besides different responses between LSMs, it was evident that longer SPI time scales better correlate with deeper-layer soil moisture anomalies. This behavior also exhibits seasonal dependence: during the rainy season (October–April), correlations between soil

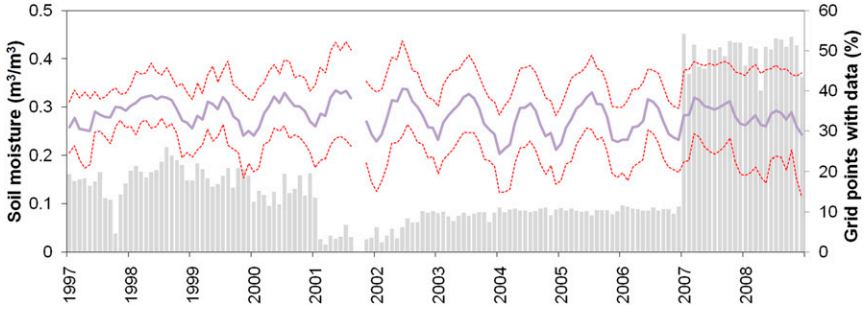

FIG. 7. SM-MW volumetric soil moisture ($m^3\ m^{-3}$; red line) temporal series, associated noise band (dotted line), and the percentage of grid pints with data for the region of SESA (gray bars) for 1997–2008.

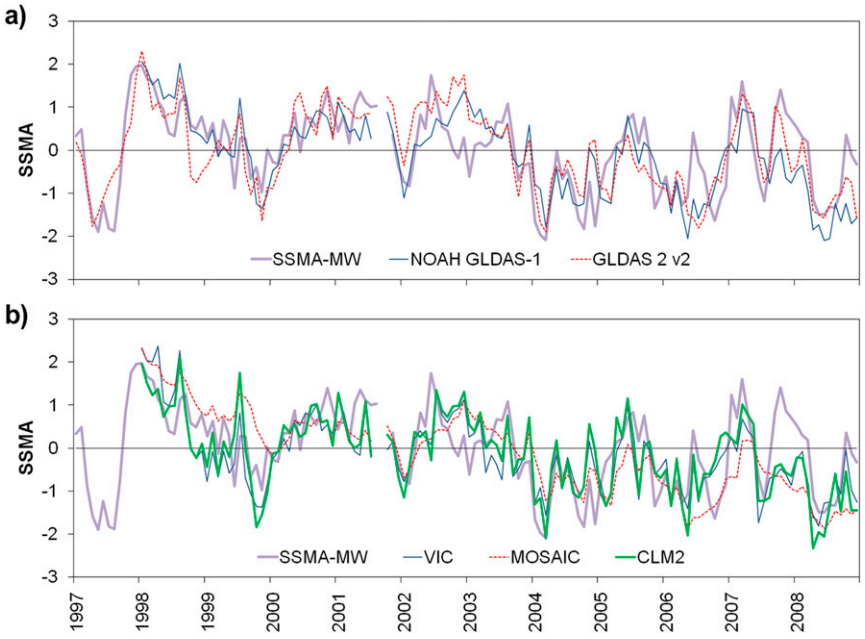

FIG. 8. SSMA for (a) SM-MW, GLDAS-2 v2, and Noah GLDAS-1; and (b) CLM2, Mosaic, VIC LSM, and SM-MW for 1997–2008.

moisture anomalies and the SPI peak at shorter time scales (e.g., around 3 and 4 months), while in winter (JJA) this maximum occurs later, generally for the SPI7. Following our interest to focus this assessment over SESA, and keeping in mind the relevance of summer and autumn agricultural production in the region, we selected the SPI3 to conduct the evaluation. A complementary assessment was carried out using the SM-MW surface soil moisture estimation for a shorter time period. In general, a good agreement was observed between simulated soil moisture and SM-MW estimations. Some LSMs, for example, the GLDAS-2 v2 (Noah) and the Noah GLDAS-1, showed the closest resemblance with SM-MW over SESA. Nevertheless, SM-MW presents considerable errors for particular time windows, related to the estimation itself and with the low percentage of grid points with data. Thus, it is difficult to infer if the differences observed are in fact due to large errors observed in SM-MW or to inadequate LSM performance.

Our first conclusion is that the GLDAS-2 dataset employing the Noah LSM is a useful tool to describe soil moisture anomalies over southern South America, but the degree of representativeness exhibits regional and seasonal dependences that should be taken into account. Comparing the results obtained from GLDAS-1 and GLDAS-2 (v1 and v2), it is clear that the precipitation dataset used to force the LSMs is of major relevance, followed by the impact of using different LSMs with equal atmospheric forcing. This result is clearly affected by our particular selection of the SPI3 as the reference dataset.

The use of simulated soil moisture values for drought research, drought monitoring, and other applications is growing steadily [e.g., Huang et al. 1996; Mo 2008; Sheffield and Wood 2008; Quan et al. 2012; Houborg et al. 2012; Pozzi et al. 2013; the Climate Prediction Center (CPC) drought monitoring]. This work shows the potential usefulness of GLDAS outputs for the analysis

TABLE 4. Correlation between the SSMAs of SM-MW and the different GLDAS LSMs (95% confidence interval). The SSMA std dev is also shown.

		LSM					
		GLDAS-1					
	SM-MW	Noah	VIC	Mosaic	CLM2	GLDAS-2	GLDAS-2 v2
Correlation	1	0.71	0.67	0.62	0.66	0.70	0.71
Std dev	0.96	0.94	0.87	0.95	0.91	0.95	0.95

of droughts and their main features (i.e., spatial distribution, frequency, and intensity) over South America but particularly over SESA. We consider that our results support the use of GLDAS for the development of new soil monitoring indices that can be applied in the context of agricultural production management.

Acknowledgments. This work was carried out with the aid of the Inter-American Institute for Global Change Research (IAI) CRN3035, which is supported by the U.S. National Science Foundation (Grant GEO-1128040); ANPCyT PICT-2010-2110; UBACyT 20020100100434; and UBACyT 01/W789. The GLDAS data used in this study were acquired as part of the mission of NASA's Earth Science Division and archived and distributed by the Goddard Earth Sciences (GES) Data and Information Services Center (DISC). The SM-MW product was made available by the CCI SM project.

REFERENCES

Adler, R. F., and Coauthors, 2003: The version-2 Global Precipitation Climatology Project (GPCP) monthly precipitation analysis (1979–present). *J. Hydrometeor.,* **4,** 1147–1167, doi:10.1175/1525-7541(2003)004<1147:TVGPCP>2.0.CO;2.

Albergel, C., and Coauthors, 2013: Skill and global trend analysis of soil moisture from reanalyses and microwave remote sensing. *J. Hydrometeor.,* **14,** 1259–1277, doi:10.1175/JHM-D-12-0161.1.

Andrade, F. H., and V. O. Sadras, Eds., 2000: *Bases para el Manejo del Maíz, el Girasol y la Soja.* INTA, 450 pp.

Balsamo, G., and Coauthors, 2012: ERA-Interim/Land: A global land surface reanalysis based on ERA-Interim meteorological forcing. ERA Rep. 13, 25 pp. [Available online at http://old.ecmwf.int/publications/library/ecpublications/_pdf/era/era_report_series/RS_13.pdf.]

Betts, A. K., 2009: Land-surface–atmosphere coupling in observations and models. *J. Adv. Model. Earth Syst.,* **1,** doi:10.3894/JAMES.2009.1.4.

Bonan, G. B., K. W. Oleson, M. Vertenstein, S. Levis, X. Zeng, Y. Dai, R. E. Dickinson, and Z.-L. Yang, 2002: The land surface climatology of the Community Land Model coupled to the NCAR Community Climate Model. *J. Climate,* **15,** 3123–3149, doi:10.1175/1520-0442(2002)015<3123:TLSCOT>2.0.CO;2.

Chen, F., and Coauthors, 1996: Modeling of land-surface evaporation by four schemes and comparison with FIFE observations. *J. Geophys. Res.,* **101,** 7251–7268, doi:10.1029/95JD02165.

Dee, D. P., and Coauthors, 2011: The ERA-Interim reanalysis: Configuration and performance of the data assimilation system. *Quart. J. Roy. Meteor. Soc.,* **137,** 553–597, doi:10.1002/qj.828.

Dirmeyer, P. A., and L. Tan, 2001: A multi-decadal global land-surface data set of state variables and fluxes. COLA Tech. Rep. 102, 43 pp. [Available online at www.iges.org/pubs/ctr_102.pdf.]

——, X. Gao, M. Zhao, Z. Guo, T. Oki, and N. Hanasaki, 2006: GSWP-2: Multimodel analysis and implications for our perception of the land surface. *Bull. Amer. Meteor. Soc.,* **87,** 1381–1397, doi:10.1175/BAMS-87-10-1381.

Dorigo, W. A., and Coauthors, 2011: The International Soil Moisture Network: A data hosting facility for global in situ soil moisture measurements. *Hydrol. Earth Syst. Sci.,* **15,** 1675–1698, doi:10.5194/hess-15-1675-2011.

——, R. de Jeu, D. Chung, R. Parinussa, Y. Liu, W. Wagner, and D. Fernández-Prieto, 2012: Evaluating global trends (1988–2010) in harmonized multi-satellite soil moisture data. *Geophys. Res. Lett.,* **39,** L18405, doi:10.1029/2012GL052988.

Hayes, M., M. Svoboda, N. Wall, and M. Widhalm, 2011: The Lincoln Declaration on Drought Indices: Universal meteorological drought index recommended. *Bull. Amer. Meteor. Soc.,* **92,** 485–488, doi:10.1175/2010BAMS3103.1.

Houborg, R., M. Rodell, B. Li, R. Reichle, and B. Zaitchik, 2012: Drought indicators based on model assimilated GRACE terrestrial water storage observations. *Water Resour. Res.,* **48,** W07525, doi:10.1029/2011WR011291.

Huang, J., H. M. Van den Dool, and K. P. Georgakakos, 1996: Analysis of model-calculated soil moisture over the United States (1931–1993) and applications to long-range temperature forecasts. *J. Climate,* **9,** 1350–1362, doi:10.1175/1520-0442(1996)009<1350:AOMCSM>2.0.CO;2.

Ji, L., and A. J. Peters, 2003: Assessing vegetation response to drought in the northern Great Plains using vegetation and drought indices. *Remote Sens. Environ.,* **87,** 85–98, doi:10.1016/S0034-4257(03)00174-3.

Kanamitsu, M., C.-H. Cheng-Hsuan, J. Schemm, and W. Ebisuzaki, 2003: The predictability of soil moisture and near-surface temperature in hindcasts of the NCEP seasonal forecast model. *J. Climate,* **16,** 510–521, doi:10.1175/1520-0442(2003)016<0510:TPOSMA>2.0.CO;2.

Kato, H., M. Rodell, F. Beyrich, H. Cleugh, E. van Gorsel, H. Liu, and T. P. Meyers, 2007: Sensitivity of land surface simulations to model physics, parameters, and forcings, at four CEOP sites. *J. Meteor. Soc. Japan,* **85A,** 187–204, doi:10.2151/jmsj.85A.187.

Koster, R. D., and M. J. Suarez, 1996: Energy and water balance calculations in the Mosaic LSM. NASA Tech. Memo. 104606, Vol. 9, 60 pp. [Available online at http://gmao.gsfc.nasa.gov/pubs/docs/Koster130.pdf.]

Krepper, C. M., and G. V. Zucarelli, 2010: Climatology of water excess and shortages in the La Plata basin. *Theor. Appl. Climatol.,* **102,** 13–27, doi:10.1007/s00704-009-0234-6.

Li, H., A. Robock, S. Liu, X. Mo, and P. Viterbo, 2005: Evaluation of reanalysis soil moisture simulations using updated Chinese soil moisture observations. *J. Hydrometeor.,* **6,** 180–193, doi:10.1175/JHM416.1.

Liang, X., D. P. Lettenmaier, E. F. Wood, and S. J. Burges, 1994: A simple hydrologically based model of land surface water and energy fluxes for GSMs. *J. Geophys. Res.,* **99,** 14 415–14 428, doi:10.1029/94JD00483.

——, ——, and ——, 1996: One-dimensional statistical dynamic representation of subgrid spatial variability of precipitation in the two-layer Variable Infiltration Capacity model. *J. Geophys. Res.,* **101,** 21 403–21 422, doi:10.1029/96JD01448.

Liu, Y. Y., W. A. Dorigo, R. M. Parinussa, R. A. M. de Jeu, W. Wagner, M. F. McCabe, J. P. Evans, and A. I. J. M. van Dijk, 2012: Trend-preserving blending of passive and active microwave soil moisture retrievals. *Remote Sens. Environ.,* **123,** 280–297, doi:10.1016/j.rse.2012.03.014.

Lloyd-Hughes, B., and M. A. Saunders, 2002: A drought climatology for Europe. *Int. J. Climatol.,* **22,** 1571–1592, doi:10.1002/joc.846.

McKee, T. B., N. J. Doesken, and J. Kleist, 1993: The relationship of drought frequency and duration to time scales. Preprints,

8th Conf. on Applied Climatology, Anaheim, CA, Amer. Meteor. Soc., 179–184.

Mo, K. C., 2008: Model-based drought indices over the United States. *J. Hydrometeor.,* **9,** 1212–1230, doi:10.1175/2008JHM1002.1.

Mueller, B., and S. I. Seneviratne, 2012: Hot days induced by precipitation deficits at the global scale. *Proc. Natl. Acad. Sci. USA,* **109,** 12 398–12 403, doi:10.1073/pnas.1204330109.

Penalba, O. C., and J. A. Rivera, 2013: Future changes in drought characteristics over southern South America projected by a CMIP5 ensemble. *Amer. J. Climate Change,* **2,** 173–182, doi:10.4236/ajcc.2013.23017.

——, ——, and V. C. Pántano, 2014: The CLARIS LPB database: Constructing a long-term daily hydro-meteorological dataset for La Plata basin, southern South America. *Geosci. Data J.,* **1,** 20–29, doi:10.1002/gdj3.7.

Pozzi, W., and Coauthors, 2013: Toward global drought early warning capability: Expanding international cooperation for the development of a framework for monitoring and forecasting. *Bull. Amer. Meteor. Soc.,* **94,** 776–785, doi:10.1175/BAMS-D-11-00176.1.

Quan, X.-W., M. P. Hoerling, B. Lyon, A. Kumar, M. A. Bell, M. K. Tippett, and H. Wang, 2012: Prospects for dynamical prediction of meteorological drought. *J. Appl. Meteor. Climatol.,* **51,** 1238–1252, doi:10.1175/JAMC-D-11-0194.1.

Robock, A., K. Y. Vinnikov, G. Srinivasan, J. K. Entin, S. E. Hollinger, N. A. Speranskaya, S. Liu, and A. Namkhai, 2000: The Global Soil Moisture Data Bank. *Bull. Amer. Meteor. Soc.,* **81,** 1281–1299, doi:10.1175/1520-0477(2000)081<1281:TGSMDB>2.3.CO;2.

——, M. Mu, K. Vinnikov, I. V. Trofimova, and T. I. Adamenko, 2005: Forty-five years of observed soil moisture in the Ukraine: No summer desiccation (yet). *Geophys. Res. Lett.,* **32,** L03401, doi:10.1029/2004GL021914.

Rodell, M., and Coauthors, 2004: The Global Land Data Assimilation System. *Bull. Amer. Meteor. Soc.,* **85,** 381–394, doi:10.1175/BAMS-85-3-381.

Rui, H., and H. Beaudoing, 2014: README document for the Global Land Data Assimilation System version 2 (GLDAS-2) products. NASA Goddard Earth Sciences Data and Information Services Center Rep., 22 pp. [Available online at ftp://hydro1.sci.gsfc.nasa.gov/data/s4pa/GLDAS/README.GLDAS2.pdf.]

Schneider, U., A. Becker, P. Finger, A. Meyer-Christoffer, B. Rudolf, and M. Ziese, 2011: GPCC Full Data Reanalysis version 6.0 at 1.0°: Monthly land-surface precipitation from rain-gauges built on GTS-based and historic data. GPCC, Offenbach, Germany, doi:10.5676/DWD_GPCC/FD_M_V6_100.

Seiler, R. A., M. Hayes, and L. Bressan, 2002: Using the standardized precipitation index for flood risk monitoring. *Int. J. Climatol.,* **22,** 1365–1376, doi:10.1002/joc.799.

Seneviratne, S. I., T. Corti, E. L. Davin, M. Hirschi, E. B. Jaeger, I. Lehner, B. Orlowsky, and A. J. Teuling, 2010: Investigating soil moisture–climate interactions in a changing climate: A review. *Earth Sci. Rev.,* **99,** 125–161, doi:10.1016/j.earscirev.2010.02.004.

Sheffield, J., and E. F. Wood, 2008: Global trends and variability in soil moisture and drought characteristics, 1950–2000, from observation-driven simulations of the terrestrial hydrologic cycle. *J. Climate,* **21,** 432–458, doi:10.1175/2007JCLI1822.1.

——, G. Goteti, and E. F. Wood, 2006: Development of a 50-yr high-resolution global dataset of meteorological forcings for land surface modeling. *J. Climate,* **19,** 3088–3111, doi:10.1175/JCLI3790.1.

Sims, A. P., D. S. Niyogi, and S. Raman, 2002: Adopting drought indices for estimating soil moisture: A North Carolina case study. *Geophys. Res. Lett.,* **29,** 1183, doi:10.1029/2001GL013343.

Szalai, S., C. Szinell, and J. Zoboki, 2000: Drought monitoring in Hungary. Early warning systems for drought preparedness and drought management, WMO/TD 1037, 182–199.

Tucker, C., and P. Sellers, 1986: Satellite remote sensing of primary production. *Int. J. Remote Sens.,* **7,** 1395–1416, doi:10.1080/01431168608948944.

Wagner, W., W. Dorigo, R. de Jeu, D. Fernandez, J. Benveniste, E. Haas, and M. Ertl, 2012: Fusion of active and passive microwave observations to create an Essential Climate Variable data record on soil moisture. *ISPRS Annals of the Photogrammetry, Remote Sensing and Spatial Information Sciences,* Vol. I-7, ISPRS, 315–321.

WMO, 2012: Standardized precipitation index user guide. WMO 1090, 24 pp. [Available online at www.wamis.org/agm/pubs/SPI/WMO_1090_EN.pdf.]

Xia, Y., J. Sheffield, M. B. Ek, J. Dong, N. Chaney, H. Wei, J. Meng, and E. F. Wood, 2014: Evaluation of multi-model simulated soil moisture in NLDAS-2. *J. Hydrol.,* **512,** 107–125, doi:10.1016/j.jhydrol.2014.02.027.

Zaitchik, B., M. Rodell, and F. Olivera, 2010: Evaluation of the Global Land Data Assimilation System using global river discharge data and a source-to-sink routing scheme. *Water Resour. Res.,* **46,** W06507, doi:10.1029/2009WR007811.